Atomic force microscopy contact, tapping, and jumping modes for imaging biological samples in liquids

F. Moreno-Herrero,[1,*] J. Colchero,[2] J. Gómez-Herrero,[1] and A. M. Baró[1]
[1]*Departamento de Física de la Materia Condensada, Facultad de Ciencias, Universidad Autónoma de Madrid, 28049 Madrid, Spain*
[2]*Departamento de Física, Facultad de Química, Universidad de Murcia, E-30100 Murcia, Spain*
(Received 24 July 2003; published 31 March 2004)

The capabilities of the atomic force microscope for imaging biomolecules under physiological conditions has been systematically investigated. Contact, dynamic, and jumping modes have been applied to four different biological systems: DNA, purple membrane, Alzheimer paired helical filaments, and the bacteriophage ϕ29. These samples have been selected to cover a wide variety of biological systems in terms of sizes and substrate contact area, which make them very appropriate for the type of comparative studies carried out in the present work. Although dynamic mode atomic force microscopy is clearly the best choice for imaging soft samples in air, in liquids there is not a leading technique. In liquids, the most appropriate imaging mode depends on the sample characteristics and preparation methods. Contact or dynamic modes are the best choices for imaging molecular assemblies arranged as crystals such as the purple membrane. In this case, the advantage of image acquisition speed predominates over the disadvantage of high lateral or normal force. For imaging individual macromolecules, which are weakly bonded to the substrate, lateral and normal forces are the relevant factors, and hence the jumping mode, an imaging mode which minimizes lateral and normal forces, is preferable to other imaging modes.

DOI: 10.1103/PhysRevE.69.031915 PACS number(s): 87.64.Dz, 07.79.Lh, 68.47.Pe, 87.14.−g

I. INTRODUCTION

Atomic force microscopy (AFM) [1] allows imaging the surface of samples on a nanometer scale in ultrahigh vacuum (UHV), ambient air, and liquids. The high resolution and the possibility to study biological systems in their native environment has created an enormous expectation on AFM as an ideal tool for molecular biology [2]. In fact, AFM has been used not only to image a variety of biological samples [3], but also to perform experiments on single molecules [4]. Even the dynamics of proteins [5], the conformational change of DNA in DNA-protein interactions [6], and the evolution of complex processes such as transcription [7] have been studied with AFM. In UHV conditions [8–11] as well as in liquids [12], true atomic resolution has been achieved. In liquids, Ohnesorge and Binnig [12] studied the possibilities of high-resolution imaging with AFM and obtained true atomic resolution images of a calcite sample immersed in water. As the authors discussed in that work, true atomic resolution is only possible due to the small tip-sample interaction present in liquids (forces as small as 10 pN are reported).

An arsenal of working modes which explore the different interaction regimes is available for AFM imaging. In UHV and in ambient air, the dynamic mode (DM-AFM), sometimes also termed the ''tapping mode'' [13,14], is the method of choice for imaging surfaces. In this AFM imaging mode, the tip is oscillated near its resonance frequency and either the reduction of the oscillation amplitude or the shift in the resonance frequency is kept constant as an image is acquired. By fine-tuning the working conditions, it is possible to operate in the noncontact regime in UHV and in ambient air. This allows surface characterization at the atomic level in UHV [15,16] and imaging molecules weakly attached to a surface in ambient air.

In the contact mode AFM (CM-AFM), the deflection of the cantilever, resulting from the mechanical contact between tip and sample, is kept constant. This imaging mode is not as flexible as the DM-AFM due to the irreversible damage produced in soft samples by the friction force between tip and sample. This could be minimized by applying low forces, but the continuous drift in the zero force level makes it extremely difficult to keep constant the total force during the scan.

The jumping mode AFM (JM-AFM) [17–19] combines features of CM-AFM and DM-AFM. In UHV, the strong adhesion force derived from the van der Waals forces and the capillary forces present in ambient air (even stronger than the van der Waals forces) make it difficult to obtain reproducible images of biomolecules using JM-AFM. In liquids, the situation is not so clear. First, van der Waals forces are very weak; second, the resonance frequency of the cantilever drops as a consequence of the large effective mass of a cantilever; and third, the high damping strongly reduces the Q factor of the system which results in a reduction of the sensitivity of the technique. Therefore, noncontact operation in liquids is very difficult, or in most cases impossible. DM-AFM becomes an intermittent contact mode similar to JM-AFM [20].

The aim of this work is to study the AFM capabilities for imaging biomolecules under physiological conditions by comparing CM-AFM, DM-AFM, and JM-AFM performances in four relevant biological samples that can be taken

*Corresponding author. Present address: Lab. Nuevas Microscopías, Fac. Ciencias, C-III, 205, Universidad Autónoma de Madrid, 28049 Cantoblanco, Madrid, Spain. Email address: fernando.moreno@uam.es

as standards. These are DNA, purple membrane (PM), Alzheimer paired helical filaments (PHF's), and the bacteriophage ϕ29. We will proceed by briefly reviewing the working principles of these AFM modes before applying them to the above-mentioned samples. Finally, we will discuss their different performances to conclude how, when, and where each mode is suitable for imaging biological samples in liquids. In particular, we shall demonstrate that JM-AFM can compete, or even overcome, dynamic mode performances for imaging individual biomolecules in a liquid environment.

II. MATERIALS AND METHODS

A. Contact mode AFM

CM-AFM was the first mode developed in AFM [1]. The working principle behind this mode is simple. The cantilever tip is brought into mechanical contact with the sample surface. A feedback mechanism measures and keeps constant the cantilever deflection (tip-surface normal force) while the tip is scanned over the surface. The image is formed by recording the voltage applied to the piezoelectric actuator in order to maintain the deflection at a fixed set point value.

This imaging mode has two clear disadvantages: first, the presence of strong lateral forces derived from the scanning motion that may produce irreversible damage on the sample; second, the technique inherently lacks a constant zero force reference level. Very often the force at the beginning of an image is quite different from that at the end of the same image because of variations in the zero force level produced by thermal drift, material creep, etc.

For imaging soft samples, small forces must be applied. This implies the use of soft cantilevers. CM-AFM images presented in this work were obtained using Olympus and nanosensor-type cantilevers of force constant in the range 0.02–0.05 N/m. Typical forces applied are about 150 pN at scan rates of three to seven lines per second.

B. Dynamic mode AFM

DM-AFM was introduced to overcome the problem of the friction force in the contact mode operation [13,14]. It is the most extended imaging mode in ambient air and in a liquid environment. When operating the AFM in this mode, the cantilever is oscillated near the free resonance frequency. Then the sample is approached to the surface until the amplitude of the cantilever is reduced to the set point value. Tip-sample interaction produces a strong amplitude reduction when the tip-sample gap is in the nanometer range. The tip is then scanned over the surface while the feedback mechanism measures and keeps constant the oscillation amplitude. So, in DM-AFM the feedback signal is the oscillation amplitude of the cantilever. This situation can be contrasted with CM-AFM, where the feedback signal is the static cantilever's deflection.

Olympus and nanosensor-type cantilevers with a force constant of 0.75 N/m were used with DM-AFM. The resonance frequency in liquid operation was 22 kHz. DM-AFM images were obtained using a typical amplitude oscillation of 2–10 nm and scan rates of three to seven lines per second.

C. Jumping mode AFM

JM-AFM combines features of CM-AFM and DM-AFM. JM-AFM works as a sequence of force versus distance curves at each point of the sampled surface with a feedback time in between. First, the tip is in contact with the surface while the feedback keeps the cantilever deflection at the set point value. Then the feedback is turned off and the tip is vertically moved away from the surface. At maximum tip-sample separation, the tip is moved laterally to the next point, avoiding lateral forces. Finally, the tip is brought again into contact with the surface. As in CM-AFM, the normal force is referred to a zero force level that may change during the scan. However, since the tip is moving in and out of contact, a simple algorithm can be used to continuously refresh the zero force level, ensuring a constant value of the set point. This feature is particularly appropriate for a careful control of the forces applied to biomolecules. Details of JM-AFM operation and imaging are given elsewhere [18,20].

Since JM-AFM is a contact technique, cantilevers with a small force constant are convenient for imaging soft samples. This is the reason why similar cantilevers to those employed in CM-AFM were chosen for operation in this mode. Typical normal forces and scan rates for this mode are 150 pN and one line per second, but we are currently improving this rate.

D. AFM sample preparation

In order to obtain reproducible images, tip-sample interaction must be chosen to be always weaker than sample-substrate interaction. While tip-sample interaction is directly related with the AFM imaging mode, sample-substrate interaction is determined by the sample preparation procedure. Hence, we stress the importance of the sample preparation method for imaging in liquids.

AFM samples have been prepared in a similar manner following the protocol described below, which can be used as a reference for other experiments performed in a liquid environment.

Freshly cleaved mica substrates (Electron Microscopy Sciences, Fort Washington, USA) are immersed for 15 min in a 0.1% dilution in water of 3-aminopropyltriethoxysilane (APTES) (Sigma-Aldrich, Alcobendas, Spain), then rinsed with 2-propanol and water, and finally dried in a gentle stream of nitrogen. At this point, a drop of the biological sample solution is placed on top of the pretreated mica for 10 min and then rinsed with the appropriate buffer. Finally, the sample is placed in the liquid cell and filled with 1 mL of the imaging buffer. DNA buffer was 20 mM Tris-Hcl (pH 7.5), 10 mM $MgCl_2$. The buffer used for bacteriophage ϕ29 and PHF's samples was 10 mM PBS (phosphate-buffered saline), pH 7.4 (Sigma-Aldrich, Alcobendas, Spain). The concentration of the molecules was adjusted by AFM inspection.

The sample preparation protocol for the PM is slightly different since no APTES mica treatment was necessary. Samples were diluted to 62 μg/mL, gently shook, sonicated, and placed on a cleaved mica substrate for 10 min. Then, PM

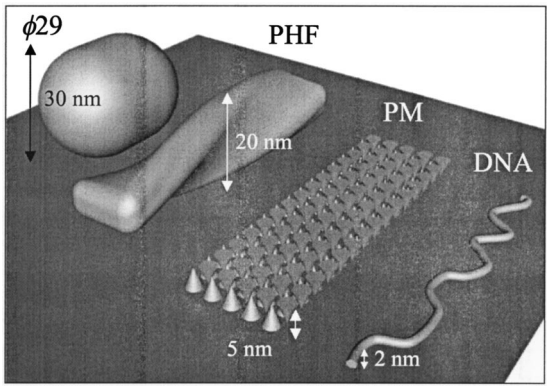

FIG. 1. Schematic of the four biological samples employed: DNA, purple membrane (PM), Alzheimer paired helical filaments (PHF's), and the bacteriophage $\phi 29$. Relative proportions are kept in the cartoon in order to stress their relative heights and the contact area of the samples with the substrate.

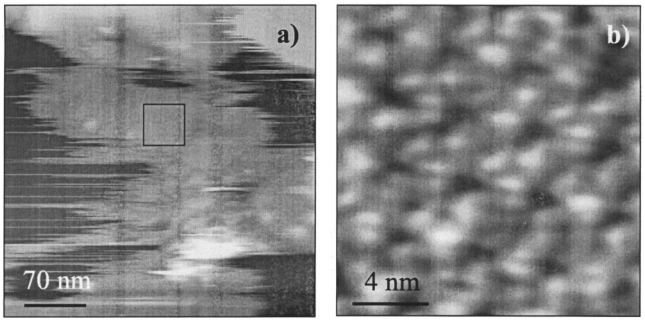

FIG. 2. Results of contact mode AFM in liquids. Only the purple membrane sample could be imaged using this technique. (Left side) A 350 nm×350 nm scan where several PM islands can be identified. Island boundaries are moved due to the high lateral forces derived from the scan. Molecular resolution can be achieved with CM-AFM as can be seen in the 14 nm×14 nm image. (Right side) The total height scale of the left side and right side images is 20 nm and 1 nm, respectively.

samples were washed with 200 mM KCl, 20 mM Tris (pH 7.8) and imaged in this buffer following [21,22]. AFM samples were never allowed to dry.

Figure 1 shows a scheme of the different samples employed in this work. The scheme was done by taking into account the relative sizes of the molecules and their substrate contact areas. Nominal heights range from 2 to 30 nm (more than one order of magnitude) and, as can be seen in Fig. 1, the effective contact areas with the substrate are quite different for the samples studied. DNA molecules can be considered as a one-dimensional wire with a large contact area relative to folded proteins. PM is typically five times higher than DNA and also has a large relative contact area. PHF particles have a typical height of 20 nm and make contact with the substrate at two points per loop [37]. Finally, $\phi 29$ particles are the highest moieties we have studied and have a small contact area since they can be thought of as globular macromolecules.

III. RESULTS

We have tested CM-AFM, DM-AFM, and JM-AFM modes in the four biological samples described above. All these results presented in this work have been obtained in solution. In all the cases, the optimum working conditions for each mode were carefully tuned. Data were obtained with a commercial microscope (Nanotec Electrónica S.L., Madrid, Spain) using an open liquid cell.

A. Contact mode

CM-AFM results are summarized in Fig. 2. CM-AFM on PM shows good intermolecular resolution in good agreement with the reported literature (Fig. 2, right side) [21]. However, the drift in the zero force level produces variations in the force applied by the cantilever. This produces substantial changes in the quality of the images. Therefore, the zero force level must be readjusted at the beginning of each image in order to obtain reproducible images. Micrometer-sized images show PM patches with undefined edges that we attribute to the motion of the islands. This is due to lateral forces induced by the scan (Fig. 2, left side). Attempts to use the contact mode, in the other samples studied, result in bad-quality images and, in most of the cases, irreversible damage to the sample.

B. Dynamic mode

DM-AFM results are shown in Fig. 3. DM-AFM images reveal regions showing molecular resolution on the purple membrane, in good agreement with previous published works [22]. In particular, the characteristic trimer structure of the sample is clearly seen in the images [Fig. 3(a), right side]. In general terms, the quality of the low-range images obtained with DM-AFM was comparable with that obtained using CM-AFM. The set point was tuned to the minimum compatible with stable operation. As commented on above, the information about the normal force applied by the tip is not directly accessible in this mode. Micron-sized images show a distribution of purple membrane areas with well-defined edges [Fig. 3(a), left side] and therefore we conclude that lateral forces are smaller in DM-AFM than in the contact mode, as expected.

DNA data acquired with DM-AFM show reproducible images with well-defined molecules [Fig. 3(b), left side]. By direct image comparison with the CM-AFM data, we deduce that the lateral forces induced by the tip when using DM-AFM are smaller than those derived from the tip contact when using CM-AFM. However, although DNA molecules are clearly defined, the average measured height of the molecules obtained with DM-AFM was much smaller than the 2-nm nominal size of double-stranded DNA. Height was measured on several points of many DNA molecules. The height histogram shows an average height of 0.6 ± 0.1 nm [Fig. 3(b), right side]. It is known that DM-AFM images of biomolecules are highly dependent on operational parameters [23,24]. In order to minimize tip-sample interaction in DM-AFM, we have employed small oscillation amplitudes. Neither acoustic nor magnetic excitation of the cantilever

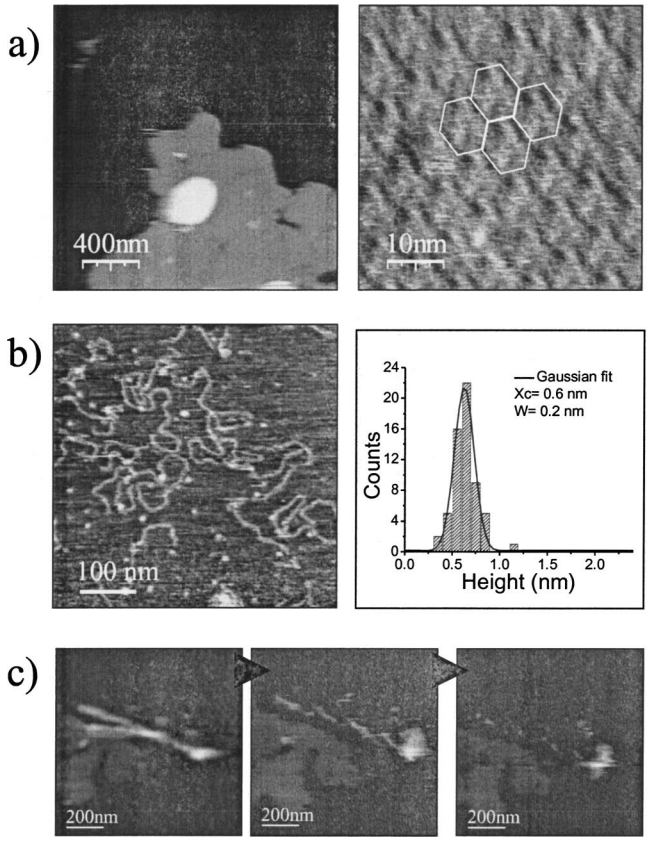

FIG. 3. Results of dynamic mode AFM in liquids. (i) Results obtained on the purple membrane. (a) Left side is a 2 μm$\times$2 μm image of a PM island. Lateral forces are smaller in DM-AFM and, hence, there is no movement of the PM islands. Molecular resolution can be obtained using this mode on the PM, as can be seen in (a), right side. The total height scale of (a) left side and (a) right side is 15 nm and 1.5 nm, respectively. (b) Results obtained on DNA. (b) Left side and (b) right side show an AFM topographic image of DNA and the corresponding height histogram. Although individual molecules can be resolved, the average height is less than half of the nominal height. (c) Results obtained on Alzheimer PHF. Three consecutive DM-AFM images of the PHF sample. There is a clear progressive molecular degradation of the imaged PHF particles.

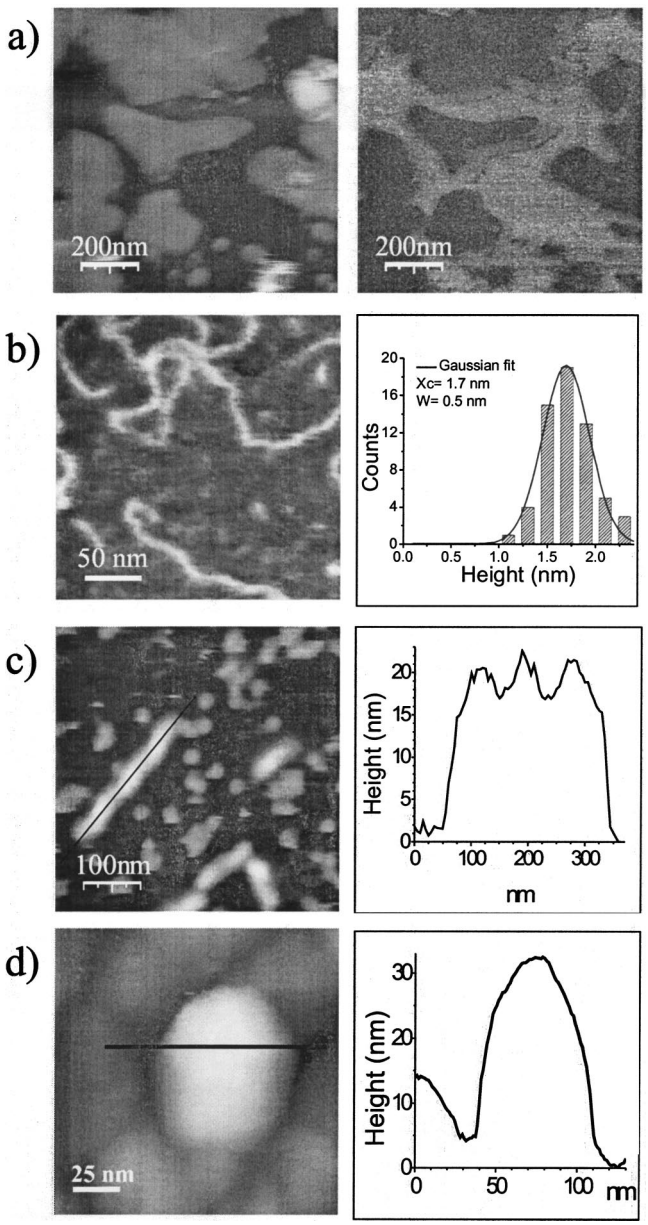

FIG. 4. Results of jumping mode AFM in liquids. (a) Results obtained on the purple membrane. (a) Left side is a 1 μm$\times$1 μm image of the PM sample. Although there is no movement of the islands induced by the scan, molecular resolution could not be achieved. Adhesion JM-AFM image [(a), right side] shows a clear contrast between the PM islands and the substrate. The total height scale of (a) left side is 15 nm. (b) Results obtained on DNA. Reproducible images of DNA molecules [(b), left side] exhibit a molecular height compatible, within the experimental error, with the nominal height of DNA [see height histogram in (b), right side]. (c) Results obtained on Alzheimer PHF. (c) Left side is a JM-AFM image of a PHF particle. Results are in good agreement with electron microscopy images since the maximum height of the molecule is about 20 nm [see (c), right side]. (d) Results obtained in the bacteriophage ϕ29. Pages could be imaged with JM-AFM but only at very low forces. Measured height is in agreement with previous published results.

resonance frequency shows any relevant differences in image quality.

Attempts to use DM-AFM in the PHF sample always result in nonreproducible and low-quality images, showing a progressive degradation of the sample with the scan [Fig. 3(c)]. The highest value of the PHF height using DM-AFM in liquids was 10 nm, but as mentioned, this value decreased after consecutive scans. Even worse results were obtained with the ϕ29 sample; the viruses are moved away by the tip scan and the images always show the mica substrate with some debris probably pertaining to ϕ29.

C. Jumping mode

JM-AFM results are shown in Fig. 4. In contrast with the other two modes, we have not achieved molecular resolution with JM-AFM on the PM sample. Micron-sized images [Fig.

4(a), left side] show a distribution of purple membrane islands with well-defined edges, so we conclude that lateral forces are smaller in JM-AFM than in the contact mode.

JM-AFM images of DNA molecules are reproducible and well defined [Fig. 4(b), left side]. DNA molecular height depends on the set point used to obtain the image (i.e., the applied force). For example, while images taken with a set point of 300 pN show a molecular height of 1.4 ± 0.3 nm, images taken at 150 pN (the minimum possible force) exhibit 1.7 ± 0.3 nm, in good agreement, within the experimental error, with the nominal height of DNA (2 nm) [height histogram in Fig. 4(b), right side].

JM-AFM images of PHF in liquids were obtained at a maximum normal force of 150 pN [Fig. 4(c), left side]. Images reveal a left-handed helical structure with an average pitch of 70 nm, in good agreement with electron microscopy published data [25,26]. We measure a variable height between 15 nm (*low* region) and 20 nm (*top* region) [Fig. 4(c), right side]. The maximum height coincides with the maximum width reported from electron microscopy images. In any helical structure, the maximum height coincides with the maximum width, and certainly our height for the *top* region is in agreement with electron microscopy data reported by others authors. Crowther [27] reported an image alternating in width between 8 and 20 nm. All these data give us good confidence about the low intrusiveness of JM-AFM when imaging in liquids. If the set point, i.e., the applied force, is increased, the height values are indeed similar to those measured with DM-AFM in liquids. Recent results show that studies of mechanical properties [28] and imaging of molecular assemblies in physiological conditions can be carried out using this imaging mode [29,30].

Finally, the bacteriophage $\phi29$ can also be imaged with JM-AFM at the minimum possible force ($\sim$150 pN) [Fig. 4(d), left side]. In this case, the characteristic parts of the virus (icosahedral capside and tail) can be resolved. Image dimensions obtained in liquids are about 35 nm$\times$60 nm $\times$110 nm (height$\times$width$\times$length) [Fig. 4(d), right side]. By direct comparison with the data obtained in air with DM-AFM (data not shown), we deduce that $\phi29$ molecules in liquids tend to be higher, narrower, and shorter (''less compressed towards the substrate''). The measured height is closer to the nominal diameter and the observed shape is also closer to that of an elongated icosahedron. Due to the small contact area of the virus with the substrate, slight increments in the tip-sample force produce the detachment of the viruses.

IV. DISCUSSION

A. Contact mode

Contact mode AFM is the technique that gives the best spatial resolution in liquids. Pioneering works showed atomic resolution on calcite, a hard surface, where the influence of lateral forces is small [12]. On the contrary, lateral force may cause irreversible damage in soft samples as biological material. Our results also suggest that contact mode is the technique that allows us to obtain the highest spatial resolution in biological samples where the presence of lateral forces is not critical, such as PM. In addition, it is the easiest to implement from a technical point of view since both DM and JM-AFM require a slight change in the experimental setup as compared to contact mode. Image acquisition in CM-AFM is fast enough to avoid thermal drift distortion. Unfortunately, CM-AFM presents high lateral forces derived from the scanning motion and therefore it is almost useless to obtain images of individual molecules. In addition, drift of the normal force signal induces a change in the zero force level that implies that the normal force is not well defined. The purple membrane is a well-known biological system that can be used as a reference sample to test the performance of the microscope. Since the quality of the images of PM obtained with the classic contact mode is comparable to published results, we conclude that the low resolution achieved on this kind of sample when using JM-AFM is not due to any technical reasons but rather to fundamental ones.

B. Dynamic mode

DM-AFM in liquids is midway between CM-AFM and JM-AFMs. DM-AFM is fast enough to obtain high-resolution images of PM, with results comparable to those obtained with contact mode. Besides, lateral forces are clearly smaller than in CM-AFM since the purple membrane islands are not moved using this technique, but probably larger than in JM-AFM since lateral and vertical motion are not synchronized. Also, since the free amplitude oscillation of the cantilever does not change during an experiment, the set point in amplitude reduction is always related with the tip-sample interaction and not with drift of zero force level, as is the case of contact mode. However, the DNA height measured with DM-AFM is smaller than that obtained with JM-AFM. In addition, the dynamic mode images show irreversible damage in PHF and cannot be used to image the $\phi29$ molecules. These results suggest that the lateral and normal forces present in DM-AFM are larger than in JM-AFM, indicating that DM-AFM operation in liquids involves tip-sample contact [31]. While in ambient air and UHV operation the strong van der Waals forces produce a well-defined minimum in the interaction potential, the screening introduced by the liquid significantly reduces this minimum. This is why contact and noncontact regimes cannot be clearly separated. In liquids, intermittent tip-sample contact takes place, resulting in a reduction in amplitude.

Another fundamental drawback of DM-AFM operation in liquids is the reduction of the Q factor of the system. This reduction is caused by the viscosity of the surrounding liquid. The relative high Q value observed in air ensures a high sensitivity since a small shift in the resonance frequency, caused by tip-sample interaction, produces a large drop in the amplitude of the oscillation. In liquids, since the resonance peak is much broader, a small shift in the resonance frequency induces a moderate change in the amplitude of oscillation. The Q of the system can be electronically increased by using a Q control [32,33]. However, we were not able to introduce significant improvements in the performance of the system using this method.

From a technical point of view, DM-AFM is more difficult to implement that CM and JM-AFM. Apart from the electronic setup, which is the same as in ambient air, oscillation of the cantilever in liquids is always more problematic. In ambient air, acoustic excitation results in a clean and well-defined frequency spectrum, with a single peak at the resonance frequency of the cantilever. The presence of the liquid environment introduces a number of spurious resonance peaks that makes DM-AFM operation more difficult. In order to avoid this problem, magnetic excitation can be used by including a coil in the AFM head and by covering the cantilevers with a ferromagnetic material [34], but this introduces additional complications such as detachment of the magnetic material from the tip, changes in the mechanical properties of the cantilever, etc.

C. Jumping mode

The experimental results show that JM-AFM is less intrusive than DM-AFM or CM-AFM. However, it has the clear drawback of a low scan rate. As commented on above, the noise of a system tends to increase as $1/f$ (f stands for frequency). Since the frequency is low, the noise is large, and the signal-to-noise ratio is poor by comparison to CM-AFM. We believe that the low acquisition rate of JM-AFM is the cause of the low quality of the high-resolution images of the purple membrane. We discard tip-sample interaction reasons to explain this fact since JM-AFM is a contact technique. To validate the hypothesis of the low scan rate, we have used CM-AFM on the PM at the same scan rate as JM-AFM and found that the molecular resolution could not be observed. Therefore, we conclude that the low lateral resolution at low scanning speed observed in JM-AFM as well as in CM-AFM is due to the higher $1/f$ noise contribution. Jumping mode requires a careful control to switch between close-loop operation and open-loop operation. Therefore, digital feedback is mandatory. We are currently using a digital signal processor to control the tip position. By careful optimization of the algorithms, the sample frequency can be increased up to 30 kHz. However, although we expect even higher speed by further improving the system, we think the JM-AFM will not be as fast as CM-AFM or DM-AFM.

JM-AFM synchronizes the lateral and vertical motion and therefore minimizes lateral forces. However, although the lateral motion of the tip is always out of contact, lateral forces are not completely eliminated since there is always an angle between the tip and the surface. If the tip-sample force is strong enough there will be a strong lateral force component derived from the normal force [35]. This is indeed the situation in ambient air where the adhesion force, mainly produced by capillary forces, always results in a strong tip-sample force. Therefore, as soon as the tip contacts the surface in ambient air, there are always high lateral forces that produce irreversible damage on the surface. The total tip-sample force (F_{tot}) is composed of two terms. First the force applied to the sample (F_{app}), which is proportional to the deflection (x) and follows the Hooke law, and second the adhesion force (F_{adh}),

$$F_{\mathrm{tot}} = F_{\mathrm{app}} + |F_{\mathrm{adh}}| = kx + |F_{\mathrm{adh}}|, \tag{1}$$

where k is the force constant of the cantilever. From Eq. (1) it is clear that when the tip snaps into the surface and the cantilever has almost zero deflection, the effective tip-sample force equals the adhesion force, which is on the order of 10 nN or even more in ambient air. However, in liquids van der Waals forces are weaker and capillary forces are not relevant any more. In these conditions, even very soft cantilevers smoothly approach a surface and the tip-sample force is only related to the cantilever deflection. In principle, using cantilevers with a very small force constant, it may be possible to apply extremely small forces. Unfortunately, the thermal noise increases as the force constant decreases, as follows from the energy equipartition theorem. Therefore, in order to achieve optimum operation, a compromise between noise and minimum forces is necessary. Small cantilevers [36] have the advantage of high-resonance frequencies in liquids. The use of small cantilevers would increase speed imaging and would reduce $1/f$ noise. The reduction of the noise would allow imaging at extremely low forces approaching the range of AFM forces to the range of optical tweezers forces.

The small adhesion force in liquids also has another benefit for JM-AFM: the tip has to be moved just a few nanometers from the sample surface to be out of contact. This results in an important increment of the JM-AFM scan rate. In ambient air operation, the distance required to avoid tip-sample contact is of the order of tens or even hundreds of nanometers (using cantilevers of about 1 N/m) and consequently the scan rate is very low. Moreover, JM-AFM uses the normal force as the feedback signal and not the amplitude reduction, as is the case of DM-AFM. This ensures images with a well-defined tip-sample force since the zero force level is continuously updated.

The good performance of JM-AFM in scanning individual biological molecules is a consequence of the different factors described in the previous paragraphs. A remarkable result is the DNA height measured in JM-AFM images, which, to our knowledge, is the highest height reported up to now. Our experiments show that as the applied force is decreased, the height of the DNA increases. Similar results are obtained with PHF. The acquisition of these data has only been possible when applying extremely low forces (less that 150 pN). The measured dimensions of these polymers are in agreement with previous published data [25]. Since some parts of the PHF particle are not in contact with the mica, imaging this type of biomolecular structure is difficult. When higher forces are applied (as in the case of DM-AFM), the structure of the PHF's suffers irreversible damage. A complete study of PHF characterization using JM-AFM in liquids can be found in [37]. We have also seen that molecules with a very weak adhesion to the substrate as the $\phi 29$ can be also measured with JM-AFM.

D. Direct comparison of dynamic mode and jumping mode

The results and the discussion presented above can be better understood in terms of the lateral and normal forces applied to the sample. Lateral forces can be divided in two types. The first type is that resulting from the scanning mo-

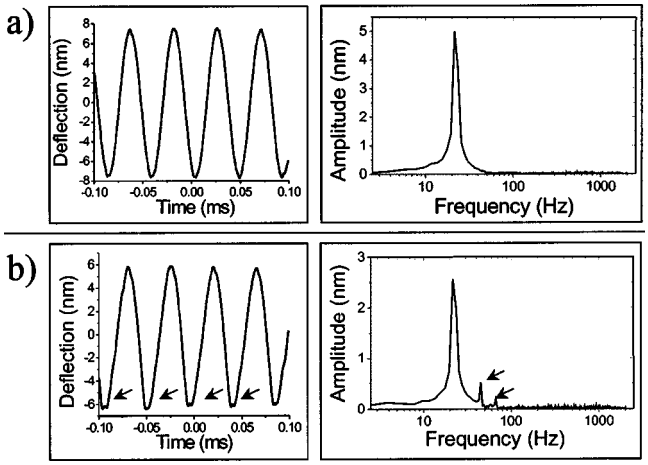

FIG. 5. Normal force signal acquired during DM-AFM in liquids. The experiment is carried out on mica using 0.75-N/m cantilevers immersed in PBS buffer. The signals are plotted in a 400-kHz bandwidth. (a) was acquired at a relatively large tip-sample distance (>300 nm) and (b) at the working (imaging) tip-sample distance. Typical parameters are 7 nm for the free cantilever amplitude, 22 kHz of resonance frequency, and 0.75 N/m of force constant. Left and right sides show, respectively, the cantilever deflection vs time and the Fourier transform. A clear difference appears when the tip is placed at the working distance (see arrows): the deflection signal is deformed at the closest tip-sample position. This fact is reflected in the Fourier transform as two peaks at 45 and 66 kHz.

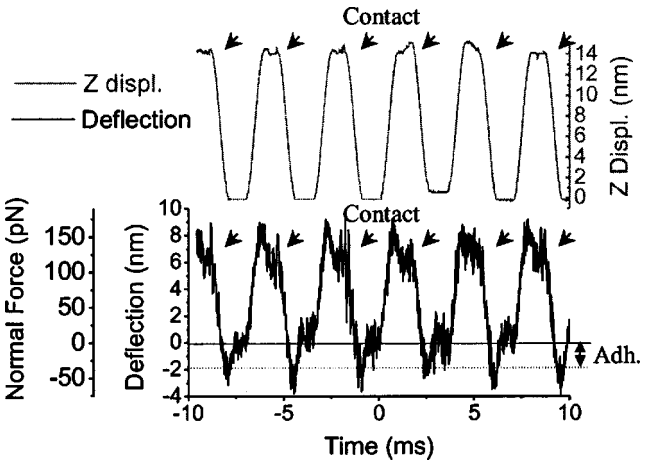

FIG. 6. JM-AFM performance in liquids. The experiment was performed on mica using 0.02-N/m cantilevers immersed in PBS buffer. The *Z* motion of the piezo and the cantilever deflection (normal force) is plotted, respectively, in the upper and in the lower part of the figure in a 100-kHz bandwidth. The JM-AFM frequency is 200 Hz. The upper part of the oscillatory signal is where the contact takes place (see arrows). From the data, a contact time of 0.85 ms is measured. During this time a normal force, within the feedback error, of 125 pN is measured. Note that an adhesion force of 30 pN is also measured.

tion (F_{LS}) itself. This lateral force appears when the tip is in contact with the sample. This happens in CM-AFM and in DM-AFM. The second kind is that resulting from the normal force depending on the surface orientation (F_{LFn}) [35]. This lateral force appears as soon as tip-sample mechanical contact takes place and can be evaluated using Eq. (2),

$$F_{\mathrm{LFn}} = F_n \sin\theta, \tag{2}$$

where F_n is the normal force (vertical deflection of the cantilever) and θ the tip-sample contact angle. Since the tip-sample angle is impossible to control with high accuracy (typically F_{LFn} is 10–30 % of F_n), efforts must be made to reduce the applied normal force. Even in DM-AFM in air, where the tip-sample forces are very weak, the effects of lateral forces resulting from the normal force have been observed [38].

The normal force is the control signal in CM-AFM and in JM-AFM. This signal is well established and it can be directly measured. Since DM-AFM operation in liquids involves contact, the effects of the tip-sample interaction are clearly reflected on the dynamic behavior of the cantilever. This allows an estimation of the average forces during imaging. To calculate this value we have recorded the deflection signal versus time at large tip-sample distances (more than 300 nm), where the short-range interactions are negligible [Fig. 5(a), left side], and at the working tip-sample distance [Fig. 5(b), left side]. The right side of Fig. 5 shows the corresponding Fourier transform of the data shown on the left side. As a consequence of the tip-sample contact, plateaus at the signal minima can be clearly seen in Fig. 5(b), left side (see arrows). The time elapsed during these plateaus is about 4.5 μs, or about 10% of the period of the signal. Therefore, the contact time of AM operation in liquids can be roughly estimated as 10% of the period oscillation. Accordingly, the average cantilever deflection due to the tip-sample contact is about 10% of the total amplitude.

In the case of Fig. 5(b), left side, this amplitude is 6 nm and, therefore, when using cantilevers of 0.75 N/m, the average force per cycle is about 1 nN. The effect of the interaction is clearly reflected in the reciprocal space as two new peaks at frequencies of 45 and 66 kHz [Fig. 5(b), right side]. These values are not related with higher resonance frequencies of the cantilever. In liquids, the maximum measured contact force in DM-AFM is larger than that applied in CM-AFM and JM-AFM. However, DM-AFM is gentler than CM-AFM since it is an intermittent contact technique. The normal force is especially destructive when imaging individual molecules because the lateral force resulting from the normal force is also large. This effect is minimized in protein crystals because an individual protein molecule is held by the surrounding proteins, which explains why molecular resolution can be achieved with DM-AFM in PM.

For direct comparison with JM-AFM performance, we have plotted the cantilever deflection signal (normal force) and the *Z* piezomovement versus time in Fig. 6. The *Z* piezo is moved 14 nm at a frequency of 200 Hz. Since for each cycle a data point is recorded, this leads to a scan rate of 200 points/s. The upper part of the oscillatory signal is where contact takes place (see arrows). The measured contact time is 0.85 ms. During that time a force, within the feedback error, of 125 pN is applied to the sample. Note that an adhesion force of 30 pN is also present in this experiment. The delay time at the furthest tip-sample position (lower part of

the plot) is related with the motion of the piezo in the X direction to the next image point. The information on the tip-sample interaction is clearly shown in Fig. 6. The adhesion force is easily available from this chart. We think that this information is also present in the contact plateau in Fig. 5(b), left side, but it is extremely difficult to extract this information from the available data.

V. CONCLUSION

In this work, we have studied the performance of different AFM imaging modes for imaging biomolecules in liquid. There is no unique scanning mode which can obtain optimum images for an arbitrary type of biological sample. Our results show that in samples with a large contact area, as is the case for the purple membrane, CM-AFM is the optimum mode. On the contrary, the CM-AFM imaging mode is almost useless when imaging individual molecular assemblies since large lateral forces result from the scan itself. In samples with individual particles weakly attached to the substrate, a precise control of the tip-sample interaction is required and then JM-AFM is the best option. Another advantage of this imaging mode is the possibility of obtaining adhesion images, information especially relevant with functionalized tips. Another advantage of JM-AFM is that no hardware implementation with respect to contact mode is needed. JM-AFM has the serious drawback of the low scanning rate, which is about one line per second. This increases the $1/f$ noise and makes it impossible to use this mode to monitor fast processes.

To follow dynamic processes of individual molecules, DM-AFM is a better option since the technique is fast and lateral forces are minimized. We have seen that DM-AFM implies normal forces of the order of ~ 1 nN and hence also large lateral forces. This would explain why we measure a low DNA height and why individual PHF particles are irreversibly damaged when using DM-AFM. The reduction of the size and force constant of the cantilevers would benefit DM-AFM because interaction forces would be lowered and JM-AFM because the scanning rate would be increased.

ACKNOWLEDGMENTS

We thank the research groups led by Professor J. Ávila, M. Salas, and A. Engel for kindly providing the PHF's, $\phi 29$, and purple membrane samples, respectively. We also thank J. Fco. Galindo for his help in the JM-AFM images of the PM sample and Ron Reifenberger for a critical reading of the manuscript. We acknowledge support from the Comunidad de Madrid for F.M.-H. This work is supported by the Ministerio de Educación y Cultura through a DGESIC Project No. BFM2001-0150, MAT2001-0664, and MAT2002-01084.

[1] G. Binnig, C. F. Quate, and C. Gerber, Phys. Rev. Lett. **56**, 930 (1986).
[2] C. Bustamante, D. A. Erie, and D. Keller, Curr. Opin. Struct. Biol. **4**, 750 (1994).
[3] C. Bustamante, C. Rivetti, and D. J. Keller, Curr. Opin. Struct. Biol. **7**, 709 (1997).
[4] M. Rief, M. Gautel, F. Oesterhelt, J. M. Fernandez, and H. E. Gaub, Science **276**, 1109 (1997).
[5] S. J. van Noort, K. O. van der Werf, A. P. Eker, C. Wyman, B. G. de Grooth, N. F. van Hulst, and J. Greve, Biophys. J. **74**, 2840 (1998).
[6] C. Rivetti, M. Guthold, and C. Bustamante, EMBO J. **18**, 4464 (1999).
[7] S. Kasas, N. H. Thomson, B. L. Smith, H. G. Hansma, X. Zhu, M. Guthold, C. Bustamante, E. T. Kool, M. Kashlev, and P. K. Hansma, Biochemistry **36**, 461 (1997).
[8] F. J. Giessibl, Science **267**, 68 (1995).
[9] S. Kitamura and M. Iwatsuki, Jpn. J. Appl. Phys., Part 2 **34**, L145 (1995).
[10] Y. Sugawara, M. Ohta, H. Veyana, and S. Morita, Science **210**, 1646 (1995).
[11] H. Veyana, M. Ohta, Y. Sugawara, and S. Morita, Jpn. J. Appl. Phys., Part 2 **34**, L1086 (1995).
[12] F. Ohnesorge and G. Binnig, Science **260**, 1451 (1993).
[13] Y. Martin, C. C. Williams, and H. K. Wickramasinghe, J. Appl. Phys. **61**, 4723 (1987).
[14] Q. Zhong, D. Inniss, K. Kjoller, and V. B. Elings, Surf. Sci. Lett. **290**, L688 (1993).
[15] F. J. Giessibl, S. Hembacher, H. Bielefeldt, and J. Mannhart, Science **289**, 422 (2000).
[16] M. A. Lantz, H. J. Hug, P. J. van Schendel, R. Hoffmann, S. Martin, A. Baratoff, A. Abdurixit, H. Guntherodt, and C. Gerber, Phys. Rev. Lett. **84**, 2642 (2000).
[17] K. O. van der Werf, C. A. J. Putman, B. G. Grooth, and J. Greve, Appl. Phys. Lett. **65**, 1195 (1994).
[18] P. J. de Pablo, J. Colchero, J. Gómez-Herrero, and A. M. Baro, Appl. Phys. Lett. **73**, 3300 (1998).
[19] A. Rosa-Zeise, E. Weilandt, S. Hild, and O. Marti, Meas. Sci. Technol. **8**, 1333 (1997).
[20] F. Moreno-Herrero, P. J. de Pablo, R. Fernández-Sánchez, J. Colchero, J. Gómez-Herrero, and A. M. Baró, Appl. Phys. Lett. **81**, 2620 (2002).
[21] D. J. Müller, D. Fontiadis, S. Scheuring, S. A. Müller, and A. Engel, Biophys. J. **76**, 1101 (1999).
[22] C. Möller, M. Allen, V. Elings, A. Engel, and D. J. Müller, Biophys. J. **77**, 1150 (1999).
[23] B. Pignataro, L. Chi, S. Gao, B. Anczykowski, C. Niemeyer, M. Adler, and H. Fuchs, Appl. Phys. A: Mater. Sci. Process. **74**, 447 (2002).
[24] A. San Paulo and R. Garcia, Biophys. J. **78**, 1599 (2000).
[25] C. M. Wischik, R. A. Crowther, M. Stewart, and M. Roth, J. Cell Biol. **100**, 1905 (1985).
[26] R. A. Crowther and C. M. Wischik, EMBO J. **4**, 3661 (1985).
[27] R. A. Crowther, Proc. Natl. Acad. Sci. USA **88**, 2288 (1991).
[28] P. J. de Pablo, I. A. T. Schaap, F. C. MacKintosh, and C. F. Schmidt, Phys. Rev. Lett. **91**, 098101 (2003).
[29] J. M. Gonzalez, M. Jimenez, M. Velez, J. Mingorance, J. M. Andreu, M. Vicente, and G. Rivas, J. Biochem. Chem. **278**, 37664 (2003).
[30] P. J. de Pablo, I. A. T. Schaap, and C. F. Schmidt, Nanotechnology **14**, 143 (2003).

[31] A. J. Putman, K. O. van der Werf, B. de Grooth, N. F. van Hulst, and J. Greve, Appl. Phys. Lett. **72**, 2454 (1994).
[32] J. Mertz, O. Marti, and J. Mlynek, Appl. Phys. Lett. **62**, 2344 (1993).
[33] J. Tamayo, A. D. L. Humphris, R. J. Owen, and M. J. Miles, Biophys. J. **81**, 526 (2001).
[34] W. Han, S. M. Lindsay, and T. Jing, Appl. Phys. Lett. **69**, 4111 (1996).
[35] F. Moreno-Herrero, P. J. de Pablo, J. Colchero, J. Gómez-Herrero, and A. M. Baró, Surf. Sci. **453**, 152 (2000).
[36] M. B. Viani, T. E. Schffer, A. Chand, M. Rief, H. E. Gaub, and P. K. Hansma, J. Appl. Phys. **86**, 2258 (1999).
[37] F. Moreno-Herrero, M. Perez, A. M. Baro, and J. Avila, Biophys. J. **86**, 517 (2004).
[38] M. S. Marcus, R. W. Carpick, D. Y. Sasaki, and M. A. Eriksson, Phys. Rev. Lett. **88**, 226103 (2002).